

# A holographic description of the Schwinger effect in a confining gauge theory

Daisuke Kawai<sup>1</sup>, Yoshiaki Sato<sup>2</sup> and Kentaroh Yoshida<sup>3</sup>

*Department of Physics, Kyoto University  
Kyoto 606-8502, Japan*

## Abstract

This is a review of the recent progress on a holographic description of the Schwinger effect. In 2011, Semenoff and Zarembo proposed a scenario to study the Schwinger effect in the context of the AdS/CFT correspondence. The production rate of quark anti-quark pairs was computed in the Coulomb phase. In particular, it provided the critical value of external electric field, above which particles are freely created and the vacuum decays catastrophically. Then the potential analysis in the holographic approach was invented and it enabled us to study the Schwinger effect in the confining phase as well. A remarkable feature of the Schwinger effect in the confining phase is to exhibit another kind of the critical value, below which the pair production cannot occur and the vacuum of the system is non-perturbatively stable. The critical value is tantamount to the confining string tension. We computed the pair production rate numerically and introduced new exponents associated with the critical electric fields.

---

<sup>1</sup>E-mail: daisuke@gauge.scphys.kyoto-u.ac.jp

<sup>2</sup>E-mail: yoshiaki@gauge.scphys.kyoto-u.ac.jp

<sup>3</sup>E-mail: kyoshida@gauge.scphys.kyoto-u.ac.jp

# Contents

<b>1</b>	<b>Introduction</b>	<b>1</b>
<b>2</b>	<b>The world-line instanton method</b>	<b>5</b>
2.1	The production rate at weak coupling . . . . .	5
2.2	The production rate at arbitrary coupling . . . . .	8
<b>3</b>	<b>The Schwinger effect in the AdS/CFT correspondence</b>	<b>11</b>
3.1	Set-up . . . . .	11
3.2	Semenoff-Zarembo's prescription . . . . .	14
<b>4</b>	<b>The Schwinger effect in a confining gauge theory</b>	<b>18</b>
4.1	Set-up . . . . .	19
4.2	Potential analysis . . . . .	20
4.3	The production rate . . . . .	24
<b>5</b>	<b>Conclusion and Discussion</b>	<b>29</b>

## 1 Introduction

The Schwinger effect [1–3] is a pair creation process in quantum electrodynamics (QED), due to an external electric field<sup>1</sup>. The production rate (per unit time and volume) is given by

$$\Gamma \sim \exp\left(-\frac{\pi m^2}{eE}\right), \quad (1.1)$$

where  $m, e$  and  $E$  are an electron mass, an elementary electric charge and an external electric field, respectively. This formula is computed under the weak electric-field ( $eE \ll m^2$ ). A typical value of  $E$  for which the Schwinger effect becomes significant is estimated as

$$E = E_{\text{Sch}} = \frac{m^2}{e} \simeq 1.3 \times 10^{18} \text{ V/m}. \quad (1.2)$$

---

<sup>1</sup> The Schwinger effect is not intrinsic to QED, but it is ubiquitous in quantum field theories coupled with a  $U(1)$  gauge field. Furthermore, it may be generalized to non-abelian gauge fields like color fields in quantum chromodynamics (QCD) [4–6].

Thus  $E_{\text{Sch}}$  is extremely large in comparison to typical values of electric field in table-top experiments. For example, a typical value of electric field necessary to ionize an atom is given by

$$E_{\text{ion}} = m^2 e^5 \alpha_s^3 \simeq 5.2 \times 10^{11} \text{ V/m}, \quad (1.3)$$

with the fine-structure constant  $\alpha_s = e^2/4\pi$ . At least so far, in real experiments, the Schwinger effect has not been observed yet, but it may be observed in the near future. The XFEL project at DESY and the ELI project in Europe plan to produce extremely strong electric field very close to  $E_{\text{Sch}}$ .

The exponential factor in the production rate indicates that the pair production process should be described as a non-perturbative phenomenon like a tunneling process in quantum mechanics. To make a virtual pair of electron and positron be real particles, it is necessary to achieve larger energy than the static energy from an external source. A phenomenological potential,

$$V_{\text{tot}}(x) = 2m - \frac{\alpha_s}{x} - eEx, \quad (1.4)$$

leads us to a tunneling picture. The potential  $V_{\text{tot}}(x)$  is composed of three parts: 1) the static electron mass, 2) the Coulomb potential with the distance  $x$  between electron and positron, and 3) an energy provided by the external electric field  $E$ . For the detail, see e.g. chapter 13 in the book [7].

The potential shapes are depicted in Fig. 1. When  $E$  is not so large, one can see the potential barrier (the blue line in Fig. 1). But the particle can penetrate it quantum mechanically, the particle creation can be described as a tunneling phenomenon. This is nothing but the Schwinger effect. It would be worth estimating the production rate roughly in the WKB sense. The triangle approximation of the potential barrier leads to the following exponential factor,

$$\Gamma \sim \exp\left(-\frac{m^2}{eE}\right).$$

This is very close to Schwinger's result (1.1), despite the rough estimation.

As  $E$  increases, the barrier tends to be lowered and at last it disappears completely at a certain value of  $E$  (the red line in Fig. 1). This value is referred to as the critical electric field  $E_c$ . The disappearance of the barrier indicates that the QED vacuum becomes

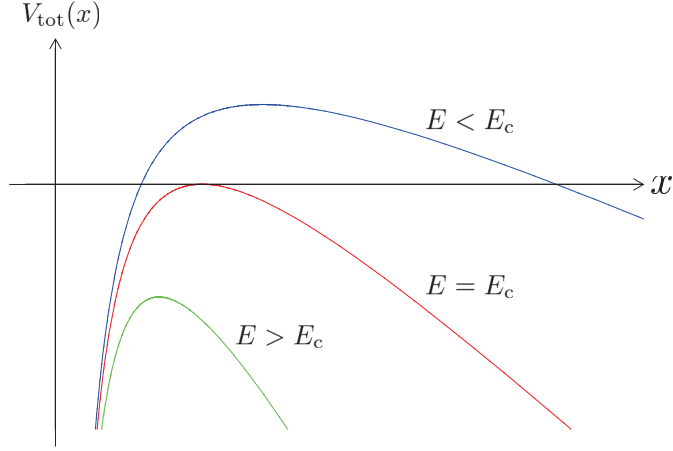


Figure 1: The potential shapes. For the blue line, the particle production is described as a tunneling process. The red line indicates that the potential barrier vanishes at a certain value  $E = E_c$  (critical electric field). For the green line, the vacuum is catastrophically unstable.

unstable catastrophically once  $E$  has reached  $E_c$ . It is easy to evaluate this value as

$$eE_c = \frac{m^2}{\alpha_s} \sim 137m^2.$$

Note that this value is far beyond the weak-field approximation  $eE \ll m^2$ . Hence, frankly speaking, it has not been clarified whether the catastrophic decay would really occur or not.

An intriguing question to be answered is “Does the catastrophic vacuum decay in QED really occur?” Although we have discussed the Schwinger effect in QED so far, let us change the direction a little here and focus upon a critical behavior in string theory. It is well known that there exists an upper critical value of electric field in the context of string theory [8, 9]. This bound obeys from a self-consistency condition of string theory. On the other hand, we know intimate relations between string theories and gauge theories. For example, these are established through the AdS/CFT duality [10–12]. According to this duality, a string theory on an anti-de Sitter (AdS) space is equivalent to a conformal field theory (CFT). The most well-studied example is the duality between type IIB string theory on  $\text{AdS}_5 \times S^5$  and the  $\mathcal{N} = 4$  supersymmetric Yang-Mills theory (SYM) with an  $SU(N)$  gauge group in four dimensions.

Thus, one may expect a connection of electric fields between the string theory and

gauge theory sides through the AdS/CFT duality. Then the result in the string-theory side suggests that the catastrophic vacuum decay can really occur at least in a class of gauge theories which have gravity duals. Thus, to investigate the possibility of the catastrophic vacuum decay in gauge theories much deeper beyond the weak-field approximation, it would be worth studying the Schwinger effect in the context of the AdS/CFT correspondence [13].

Another motivation is to argue the Schwinger effect in QCD. It may give rise to a new mechanism of a confinement/deconfinement phase transition and it would have a connection with the RHIC and LHC experiments, where strong electro-magnetic fields and color fields are induced due to the collision of heavy ions. It motivates us to study the Schwinger effect in confining gauge theories. However, it is not easy to tackle this issue with the standard method in quantum field theories. A nice way is to employ a holographic computation by realizing confining gauge theories with appropriate D-brane set-ups. In fact, we have considered the Schwinger effect in confining gauge theories along this line [14–16]. The potential analysis [14, 15] has been done for general confining backgrounds [17–19] by generalizing the procedure in the Coulomb phase [20]. The production rate has been evaluated numerically in the case of a confining D3-brane background [16] (which is an example of AdS solitons [21]).

The organization of this review is as follows. Section 2 gives a short review of the world-line instanton method based on articles [22–24]. This is a method to calculate the production rate and becomes a key ingredient in preparing a holographic computation in the subsequent sections. In section 3, we consider the Schwinger effect in the  $\mathcal{N} = 4$  SYM. This system is conformal and contains no fundamental matter field. Hence, naively, the Schwinger effect cannot be argued. A possible way of overcoming these points is to employ the Higgs mechanism. We first compute the production rate in the Higgsed  $\mathcal{N} = 4$  SYM naively by using the world-line instanton method. After all, this computation leads to a puzzle on the critical value of external electric field. Then, to resolve this puzzle, an improved holographic set-up is presented by following the seminal work by Semenoff and Zarembo [13]. The production rate is reconsidered along this line and the puzzle is certainly resolved. Section 4 is the main part of this article based on a series of our works [14–16] and investigates the Schwinger effect in a confining gauge theory by employing a confining D3-brane background [21]. A remarkable feature is

that there is another kind of critical value of electric field due to the existence of the confining phase. We have evaluated the production rate numerically and computed new exponents associated with the critical electric fields. Section 5 is devoted to conclusion and discussion.

## 2 The world-line instanton method

In this section, we will give a short review of the world-line instanton method by following the works [22–24].

### 2.1 The production rate at weak coupling

There are various methods to calculate the pair production rate of the Schwinger effect in QED. We shall introduce here one of them, called the world-line instanton method. An advantage of this method is that one can easily add a contribution coming from the Coulomb potential. In particular, it enables us to compute the production rate at arbitrary coupling. In the following, we will explain first the computation at weak coupling, then the one at arbitrary coupling.

As a simple example, let us first consider a massive scalar QED. The action for a massive scalar QED (in the Euclidean signature) is

$$S = \int d^4x \left( \frac{1}{4} F_{\mu\nu}^2 + |D_\mu \phi|^2 + m^2 |\phi|^2 \right) \quad (2.1)$$

with the covariant derivative,

$$D_\mu = \partial_\mu + ieA_\mu + ieA_\mu^{\text{ex}}. \quad (2.2)$$

Note here that the vector field is divided into a dynamical (fluctuating) part  $A_\mu$  and an external part  $A_\mu^{\text{ex}}$ . The path integration is performed only for the dynamical part, not for the external part.

The production rate  $\Gamma$  is given by the imaginary part of the vacuum energy density  $\varepsilon_0$ ,

$$\Gamma = 2 \text{Im} \varepsilon_0 = -\frac{2}{V_4} \text{Im} \log \int \mathcal{D}A \mathcal{D}\phi e^{-S}. \quad (2.3)$$

Here  $V_4$  is the volume of the four dimensional space. By performing the path integral for the scalar field  $\phi$ , the following expression is obtained,

$$V_4\Gamma = -2 \text{Im} \log \int \mathcal{D}A \exp \left( - \int d^4x \frac{1}{4} F_{\mu\nu}^2 - \text{tr} \log (-D^2 + m^2) \right). \quad (2.4)$$

In a small coupling region, the dynamical part of the vector field can be ignored. Hence the expression (2.4) is approximated as

$$V_4\Gamma \simeq -2 \text{Im} \int_0^\infty \frac{dT}{T} \int \mathcal{D}x \exp \left( -\frac{1}{2T} \int_0^1 d\tau \dot{x}^2 - \frac{m^2 T}{2} + ie \int_0^1 d\tau A_\mu^{\text{ex}} \dot{x}_\mu \right). \quad (2.5)$$

Here we have used Schwinger's parametrization

$$\log \alpha = - \int_0^\infty \frac{dt}{t} e^{-\alpha t}$$

and the quantum-mechanical path-integral representation. Note that  $x_\mu(\tau)$  satisfies the periodic boundary condition  $x_\mu(0) = x_\mu(1)$ .

Next, as for the expression (2.5), the  $T$ -integration is firstly performed, and then the integral for  $x(\tau)$  is done<sup>2</sup>. For later convenience, let us suppose that

$$m \sqrt{\int_0^1 d\tau \dot{x}^2} \gg 1. \quad (2.6)$$

This condition (2.6) will be identified with the weak-field condition for the external electric field, as we will see later. It is worth noting that the integration about  $T$  can be regarded as a modified Bessel function,

$$K_0(x) = \frac{1}{2} \int_0^\infty \frac{dt}{t} \exp \left( -t - \frac{x^2}{4t} \right)$$

and its asymptotic behavior for large  $x$  is

$$K_0(x) \simeq \sqrt{\frac{\pi}{2x}} e^{-x}. \quad (2.7)$$

Then, under the condition (2.6), the expression (2.5) is simplified as

$$V_4\Gamma = -2 \text{Im} \int \mathcal{D}x \frac{1}{m} \sqrt{\frac{2\pi}{T_0}} \exp(-S_{\text{particle}}), \quad (2.8)$$

where  $S_{\text{particle}}$  and  $T_0$  are defined as

$$S_{\text{particle}} \equiv m \sqrt{\int_0^1 d\tau \dot{x}^2} - ie \int_0^1 d\tau A_\mu^{\text{ex}} \dot{x}_\mu, \quad (2.9)$$

---

<sup>2</sup> The integrations in the opposite order lead to the Heisenberg-Euler Lagrangian [2].

$$T_0 \equiv \frac{\sqrt{\int d\tau \dot{x}^2}}{m}. \quad (2.10)$$

The above computation is identical with the method of steepest descent for the  $T$ -integration. But, note that the condition (2.6) is not necessary if we do not want to use the asymptotic form of the Bessel function at this stage.

The path integral about  $x(\tau)$  is evaluated by the method of steepest descent. The equation of motion obtained from  $S_{\text{particle}}$  is

$$\frac{m\ddot{x}_\mu}{\sqrt{\int d\tau \dot{x}^2}} = -ieF_{\mu\nu}\dot{x}_\nu. \quad (2.11)$$

Multiplying (2.11) by  $\dot{x}_\mu$  and integrating it, we find the following relation,

$$\dot{x}^2 \equiv a^2 \quad (\text{constant}). \quad (2.12)$$

Let us suppose a constant electric field is turned on the  $x_1$ -direction. Then the vector potential is taken as

$$A_1^{\text{ex}}(x_0) = -iEx_0. \quad (2.13)$$

The other components are set to be zero. Note that the imaginary unit  $i$  appears because we are now working in the Euclidean signature.

With the constant electric field, the classical solutions are represented by

$$x_0 = \frac{m}{eE} \cos\left(\frac{aeE}{m}\tau\right), \quad x_1 = \frac{m}{eE} \sin\left(\frac{aeE}{m}\tau\right), \quad x_2 = x_3 = 0. \quad (2.14)$$

The periodic boundary condition  $x_\mu(0) = x_\mu(1)$  determines  $a$  like

$$\frac{aeE}{m} = 2n\pi, \quad n \in \mathbb{N}. \quad (2.15)$$

Thus the classical motion has been completely fixed. This solution is often called ‘‘instanton,’’ just because this is a classical solution in the Euclidean signature.

With the relation (2.15), it is easy to check that the assumption (2.6) is nothing but the weak-field condition

$$E \ll E_{\text{Sch}}, \quad (2.16)$$

as noted before. Furthermore, the assumption is the same as the condition to ensure that the steepest-descent method is a good approximation.



By combining the classical action

$$S_{\text{cl}}^{(n)} = \frac{\pi m^2 n}{eE}$$

with one-loop prefactors, the production rate is evaluated as

$$\Gamma = \frac{(eE)^2}{(2\pi)^3} \sum_{n=1}^{\infty} \frac{(-1)^{n+1}}{n^2} \exp\left(-\frac{\pi m^2}{eE} n\right). \quad (2.17)$$

The production rate (2.17) is the same as the Schwinger formula for the scalar QED. This expression is valid at small coupling and under the weak-field condition. The method presented here is applicable to a spinor QED as well [23].

We have not explained the one-loop prefactor here. For the detail of the derivation, for example, see the works [22, 24].

## 2.2 The production rate at arbitrary coupling

Let us generalize the production rate (2.17) at weak coupling to the one at arbitrary coupling, though we still suppose the weak-field condition.

Before going to the detail, it is worth to see a heuristic argument based on the pair production rate of monopole and anti-monopole. In the Georgi-Glashow model, it is evaluated as [25]

$$\Gamma = \frac{(gB)^2}{(2\pi)^3} \exp\left(-\frac{\pi M^2}{gB} + \frac{g^2}{4}\right), \quad (2.18)$$

where  $B$ ,  $M = 4\pi m/e^2$  and  $g = 4\pi/e$  are an external magnetic field, a monopole mass and a magnetic charge, respectively. This result (2.18) is valid under the following two conditions:

$$g^2 \gg 1, \quad gB \ll M^2.$$

Let us perform electric-magnetic duality for the above result. The production rate is mapped to

$$\Gamma = \frac{(eE)^2}{(2\pi)^3} \exp\left(-\frac{\pi m^2}{eE} + \frac{e^2}{4}\right). \quad (2.19)$$

But the validity region is

$$e^2 \gg 1, \quad eE \ll m^2,$$

and the strong coupling region is supposed as opposed to the previous computation. This observation indicates the expression (2.19) should be valid for arbitrary coupling. In fact, this expression can be obtained by a direct computation [22], as we will show below.

In the previous subsection, the coupling constant has been supposed to be so small that the dynamical field  $A_\mu$  is ignorable. But we will take account of  $A_\mu$  at finite coupling here. Then the equation (2.4) is replaced by

$$V_4\Gamma = -2 \text{Im} \log \left\langle \exp \left[ -\text{tr} \log \left( -(\partial + ieA + ieA^{\text{ex}})^2 + m^2 \right) \right] \right\rangle, \quad (2.20)$$

where the expectation value is defined as

$$\langle g(A) \rangle \equiv \frac{\int \mathcal{D}A \exp \left( -\frac{1}{4} \int d^4x F^2 \right) g(A)}{\int \mathcal{D}A \exp \left( -\frac{1}{4} \int d^4x F^2 \right)}. \quad (2.21)$$

Furthermore, the equation (2.20) can be approximated as

$$V_4\Gamma \simeq 2 \text{Im} \left\langle \text{tr} \log \left( -(\partial + ieA + ieA^{\text{ex}})^2 + m^2 \right) \right\rangle \quad (2.22)$$

under the weak-field condition. This can be regarded as an electron loop expansion in the Feynman diagrams.

Here we keep the diagrams with a single electron loop and drop off the higher-loop contributions. This selection is a good approximation when the external field is weak enough. By doing the same calculation as in the previous subsection, the production rate is obtained as

$$\begin{aligned} V_4\Gamma &= -2 \text{Im} \int_0^\infty \frac{dT}{T} \int \mathcal{D}x \exp \left( -\frac{1}{2T} \int_0^1 d\tau \dot{x}^2 - \frac{m^2 T}{2} + ie \oint A_\mu^{\text{ex}} dx_\mu \right) \\ &\times \left\langle \exp \left( ie \oint A_\mu dx_\mu \right) \right\rangle. \end{aligned} \quad (2.23)$$

In comparison to (2.5), the expression (2.23) includes the contribution coming from the Coulomb interaction. This modification is reflected as a  $U(1)$  Wilson loop in (2.23).

Under the condition (2.6), the integration about  $T$  leads to

$$V_4\Gamma \simeq -2 \text{Im} \int \mathcal{D}x \frac{1}{m} \sqrt{\frac{2\pi}{T_0}} \exp \left( -S_{\text{particle}} - \frac{e^2}{8\pi^2} \oint \oint \frac{dx \cdot dy}{(x-y)^2} \right), \quad (2.24)$$

where we have employed the following identity:

$$\left\langle \exp \left( ie \oint A_\mu dx_\mu \right) \right\rangle = \exp \left( -\frac{e^2}{8\pi^2} \oint \oint \frac{dx \cdot dy}{(x-y)^2} \right). \quad (2.25)$$

The derivation of (2.25) is straightforward.

Let us next perform the path-integral about  $x(\tau)$ . The Coulomb interaction should change classical solutions, as a matter of course. However, note here that the Coulomb interaction term is invariant under a scale transformation and a rotation in the plane on which the instanton is rotating. Hence it does not depend on the size of the classical solutions. Thus the classical solutions are not changed when the Wilson loop is added as a perturbation.

The classical action is modified as

$$S_{\text{cl}}^{(n)} = \left( \frac{\pi m^2}{eE} - \frac{e^2}{4} \right) n. \quad (2.26)$$

Here we have used the formula

$$-\frac{e^2}{8\pi^2} \oint \oint \frac{dx \cdot dy}{(x-y)^2} = n \frac{e^2}{4}, \quad (2.27)$$

where an unphysical divergence has been ignored.

Recall that the contributions of the Coulomb interaction are small. Then the prefactor of the exponential has not been modified. As a result, the production rate is given by

$$\Gamma = \frac{(eE)^2}{(2\pi)^3} \sum_{n=1}^{\infty} \frac{(-1)^{n+1}}{n^2} \exp \left( - \left( \frac{\pi m^2}{eE} - \frac{e^2}{4} \right) n \right). \quad (2.28)$$

Thus we have reproduced the conjectured form (2.19) as the  $n = 1$  case.

Note that the production rate is not exponentially suppressed any more just after  $E$  has reached the critical value

$$E = E_c \equiv \frac{4\pi m^2}{e^3}.$$

That is, the vacuum becomes unstable catastrophically above this critical value. However, the weak-field condition  $E \ll E_{\text{Sch}}$  is broken as follows:

$$E_c = \frac{E_{\text{Sch}}}{\alpha_s} \implies E_c \sim 137 E_{\text{Sch}}.$$

Hence it is not certain whether the catastrophic vacuum decay really occurs or not. It is significant to answer this question. A possible way is to follow a holographic computation, as we will introduce in the next section.

### 3 The Schwinger effect in the AdS/CFT correspondence

In this section, we will consider the Schwinger effect in the context of the AdS/CFT correspondence. There are many variations of AdS/CFT, but we will concentrate on the most typical example, the duality between type IIB superstring on  $\text{AdS}_5 \times S^5$  and the  $\mathcal{N} = 4$   $SU(N)$  SYM in four dimensions. However, in order to argue the Schwinger effect, there are three obstacles:

1. The  $\mathcal{N} = 4$   $SU(N)$  SYM is conformal (i.e., all of the fields are massless).
2. All of the matter fields belong to the adjoint representation.
3. There is no  $U(1)$  gauge field.

As for (3), as a matter of course, one may consider non-abelian Schwinger effects. But it is not so easy to study the issue itself. Hence it is better to focus upon an abelian Schwinger effect as a first trial.

Let us first introduce a  $U(1)$  gauge field and fundamental matter fields by employing the Higgs mechanism. Then one can compute the pair production rate of the fundamental matter fields by following the procedure introduced in Sec. 2. However, we will encounter a puzzle for the critical value of electric field. To resolve it, Semenoff and Zarembo proposed a prescription [13] and presented an improved holographic set-up<sup>3</sup>. Subsection 3.2 will introduce their proposal.

#### 3.1 Set-up

We start from the  $\mathcal{N}=4$   $SU(N+1)$  SYM theory. It consists of a gauge field  $\hat{A}_\mu$  ( $\mu = 0, \dots, 3$ ), six real scalar fields  $\hat{\Phi}_I$  ( $I = 1, \dots, 6$ ) and four Weyl fermions  $\hat{\Psi}$ , the hat is attached for later convenience. All of the fields belong to an adjoint representation of  $SU(N+1)$ . One should notice here that the  $\mathcal{N} = 4$  SYM includes neither a  $U(1)$  gauge field and nor fundamental matters.

---

<sup>3</sup> For an earlier trial, see the work [26]. In Ref. [27], it has been shown that an electric field creates a pair production current on a probe brane at zero temperature. The finite-temperature case is discussed in Refs. [28, 29].

Then, by breaking  $SU(N+1)$  to  $SU(N) \times U(1)$  with the Higgs mechanism, let us introduce a  $U(1)$  gauge field. The  $SU(N+1)$  fields are decomposed into the  $SU(N)$  part, the  $U(1)$  part and non-diagonal parts:

$$\hat{A}_\mu = \begin{pmatrix} A_\mu & \omega_\mu \\ \omega_\mu^\dagger & a_\mu \end{pmatrix}, \quad \hat{\Phi}_I = \begin{pmatrix} \Phi_I & \omega_I \\ \omega_I^\dagger & m\theta_I + \phi_I \end{pmatrix}, \quad \hat{\Psi} = \begin{pmatrix} \Psi & \chi \\ \chi^\dagger & \psi \end{pmatrix}. \quad (3.1)$$

Here  $A_\mu$  [ $a_\mu$ ],  $\Phi_I$  [ $\phi_I$ ], and  $\Psi$  [ $\psi$ ] are the  $SU(N)$  [ $U(1)$ ] gauge, the scalar and the fermionic fields, respectively. The vacuum expectation value (VEV) of the scalar fields is supposed to be

$$\langle \hat{\Phi}_I \rangle = \text{diag}(0, \dots, 0, m\theta_I), \quad \sum_{I=1}^6 \theta_I^2 = 1.$$

In terms of D-branes, the Higgs mechanism corresponds to separating a single D3-brane from the remaining stuck of  $N$  parallel D3-branes. The distance between the separated D3-brane and the  $N$  D3-branes is related to the VEV of the scalar fields.

As a result, the  $\mathcal{N}=4$   $SU(N+1)$  SYM action  $S_{\mathcal{N}=4\text{SYM}}^{SU(N+1)}$  is decomposed like

$$S_{\mathcal{N}=4\text{SYM}}^{SU(N+1)} = S_{\mathcal{N}=4\text{SYM}}^{SU(N)} + S_{\mathcal{N}=4\text{SYM}}^{U(1)} + S_W.$$

Here  $S_W$  is the action for the W-boson supermultiplet

$$S_W = \frac{1}{g_{\text{YM}}^2} \int d^4x \left[ (D_\mu \omega_I)^\dagger D^\mu \omega_I + \omega_I^\dagger (\Phi_K - m\theta_K)^2 \omega_I - m^2 \omega_I^\dagger \theta_I \theta_J \omega_J + \dots \right]. \quad (3.2)$$

For our purpose, we will concentrate on the complex scalar fields  $\omega_I$  (called ‘‘quarks’’) and drop off the vector field  $\omega_\mu$  and the fermionic field  $\chi$  in the W-boson supermultiplet. The higher order interactions are also ignored.

A remarkable point is that the covariant derivative  $D_\mu$  in (3.2) is given by

$$D_\mu = \partial_\mu + ia_\mu - iA_\mu.$$

Thus the scalar fields in the W-boson supermultiplet have a finite mass  $m$  and couple to the  $U(1)$  gauge field  $a_\mu$  as well as the  $SU(N)$  gauge field  $A_\mu$ .

Note here that five scalar fields are massive but one scalar field is massless. For example, let us consider the case with  $\theta_I = (0, 0, 0, 0, 0, 1)$ . For  $I = 1, \dots, 5$ , mass terms exist in the action (3.2), but for  $I = 6$  it vanishes. The massless field is absorbed into the vector field  $\omega_\mu$  as the longitudinal mode so that  $\omega_\mu$  becomes massive.

Let us calculate the pair production rate<sup>4</sup> for  $\omega_I$  by using the world-line instanton method. In the following, we take the 't Hooft limit [30] where  $N \rightarrow \infty$  with  $\lambda \equiv g_{\text{YM}}^2 N$  fixed. The value of  $\lambda$  is also supposed to be sufficiently large so as to suppress the dynamical part of the  $U(1)$  gauge field. Then  $a_\mu$  can be regarded as an external field like

$$a_1^{\text{ex}} = -iEx_0 \quad (\text{the other components are zero}). \quad (3.3)$$

Note that we work in the Euclidean signature to calculate the production rate.

Then the production rate can be evaluated as<sup>5</sup>

$$V_4\Gamma = -5N \text{Im} \int \mathcal{D}x g[x(\tau)] \exp\left(-m \int_0^1 d\tau \sqrt{\dot{x}^2} - i \int_0^1 d\tau a_\mu^{\text{ex}} \dot{x}_\mu\right) \langle W[x] \rangle, \quad (3.4)$$

$$W[x] = \text{tr}_{SU(N)} \exp\left(\int_0^1 d\tau \left(iA_\mu \dot{x}_\mu + \Phi_K \theta_K \sqrt{\dot{x}^2}\right)\right), \quad (3.5)$$

where  $g[x(\tau)]$  is a functional of  $x(\tau)$  and does not contribute to the exponential factor in the production rate. In the derivation of (3.4), we have assumed that quark mass is very heavy, and the external electric field is weak,  $E \ll m^2$ .

It would be helpful to comment on some differences between (2.8) and (3.4). Since the production rate is proportional to the number of fundamental particles,  $5N$  appears in (3.4) (note that one of  $\omega_I$  has been eaten by  $\omega_\mu$ ). The kinetic term for the instanton is changed, but this change does not affect the exponential factor in the leading-order computation. Note also that  $W[x]$  in (3.4) is a supersymmetric  $SU(N)$  Wilson loop [34,35] because the  $SU(N)$  gauge field  $A_\mu$  has been regarded as a dynamical field.

Now it is necessary to evaluate the VEV of the Wilson loop. One can compute it by examining the area of the minimal surface of a string attaching to the circle. The result at strong coupling is given by [33,36]

$$\langle W[x] \rangle = e^{\sqrt{\lambda}},$$

---

<sup>4</sup> Recall that  $\omega_I$ ,  $\omega_\mu$  and  $\chi$  have the same mass. Hence  $\omega_I$ ,  $\omega_\mu$  and  $\chi$  may be produced equally. In fact, the exponential factor does not depend on spins, though the prefactors are different. In addition, as for  $\omega_\mu$ , there is another kind of problem called the Nielsen-Olsen instability. When  $\omega_\mu$  pairs are created under external electric and magnetic fields. See the work [31] for the detail of this instability in the holographic Schwinger effect.

<sup>5</sup>For the detailed derivation, see sec. 2 in the work [32]. It is basically the same as the derivation of a supersymmetric Wilson loop in an earlier work [33], up to prefactors.

by supposing that the mass of quarks should be very heavy. Then the exponential factor in the production rate is evaluated as

$$\Gamma \sim e^{-S_{\text{cl}}} = \exp\left(-\frac{\pi m^2}{E} + \sqrt{\lambda}\right). \quad (3.6)$$

This is an expected form because  $\sqrt{\lambda}$  is regarded as a coupling constant in the large  $N$  gauge theory [34, 35]. From (3.6), one can read off the critical electric field,

$$E_c = \frac{\pi m^2}{\sqrt{\lambda}}. \quad (3.7)$$

When  $E < E_c$ , the pair production is suppressed exponentially. When  $E > E_c$ , the vacuum becomes unstable catastrophically.

It may seem that the critical electric field (3.7) satisfies the weak-field condition because  $\lambda$  is supposed to be very large. However, it would be unlikely that heavy particles are produced due to the Schwinger effect because such a process is severely suppressed. Hence the above computation may be unsatisfactory.

In addition, note that the critical electric field (3.7) does not agree with the one obtained from the DBI action of a D3-brane sitting near the AdS boundary<sup>6</sup>,

$$E_c^{\text{DBI}} = \frac{2\pi m^2}{\sqrt{\lambda}}. \quad (3.8)$$

This disagreement may lead to a puzzle.

In the next subsection, we will introduce a nice prescription to resolve the above two points simultaneously.

## 3.2 Semenoff-Zarembo's prescription

In the work [13], Semenoff and Zarembo proposed a holographic set-up to study the Schwinger effect in the higgsed  $\mathcal{N} = 4$  SYM.

The set-up is the following. A single D3-brane is separated from the stack of  $N$  parallel D3-branes. The near-horizon limit of the stack of  $N$  D3-branes is represented by the  $\text{AdS}_5 \times S^5$  geometry:

$$ds^2 = g_{MN} dx^M dx^N$$

---

<sup>6</sup> If the D3-brane is located at the boundary, then the mass  $m$  diverges. Hence  $m$  has become finite by slightly separating the D3-brane from the boundary.

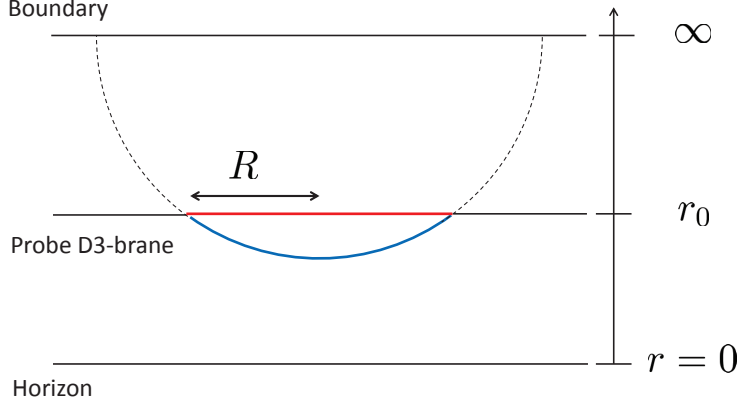


Figure 2: The location of the probe D3-brane and the configuration of the string world-sheet.

$$= \frac{r^2}{L^2} dx_\mu dx^\mu + \frac{L^2}{r^2} dr^2 + L^2 d\Omega_5^2, \quad (3.9)$$

where  $L = \lambda^{1/4} \sqrt{\alpha'}$  is the curvature radius. The coordinates  $x^M$  ( $M = 0, \dots, 9$ ) describe the ten-dimensional spacetime and  $x^\mu$  ( $\mu = 0, \dots, 3$ ) represent the four-dimensional spacetime in which the dual gauge theory lives. The coordinate  $r$  is the radial direction of the AdS space. The horizon of AdS is located at  $r = 0$  and the conformal boundary is at  $r = \infty$ . The separated D3-brane can be treated as a probe brane in the bulk AdS. A remarkable point is that the probe D3-brane is put at an intermediate position ( $r = r_0$ ) between the horizon and the boundary, and it sits at a point on  $S^5$ . For the configuration, see Fig. 2.

According to the set-up, the mass of a single quark is not infinite any more but finite. The quark mass is measured by the energy of a string stretched from the probe D3-brane to the horizon like

$$m = T_F r_0. \quad (3.10)$$

Here  $T_F = 1/2\pi\alpha'$  is the string tension.

Inspiring from the fact that a circular Wilson loop appears in the production rate (3.4), Semenoff and Zarembo proposed a new scenario that the production rate may be computed by a circular Wilson loop on the probe D3-brane equipped with a constant electric  $B$ -field. The VEV of the Wilson loop can be evaluated by the area of a minimal surface of the fundamental string attaching to the boundary loop. That is, the exponential factor in the production rate is estimated as

$$\Gamma \sim \exp(-S_{\text{NG}} - S_{B_2}). \quad (3.11)$$



Here  $S_{\text{NG}}$  and  $S_{B_2}$  are the Nambu-Goto (NG) action and the coupling to an NS-NS 2-form. In the Euclidean signature, these quantities are given by, respectively,

$$S_{\text{NG}} = T_{\text{F}} \int d^2\sigma \sqrt{\det G_{\alpha\beta}}, \quad (3.12)$$

$$S_{B_2} = -T_{\text{F}} \int d^2\sigma B_{MN} \partial_\tau x^M \partial_\sigma x^N. \quad (3.13)$$

The string world-sheet is parametrized by  $\sigma^\alpha = (\tau, \sigma)$ . Then  $G_{\alpha\beta}$  is the induced metric and  $B_{MN}$  is an anti-symmetric two-form flux. Note again that we work in the Euclidean signature for both the bulk spacetime and the world sheet.

It would be worth comparing the world-line instanton method and Semenoff-Zarembo's prescription. Recall that in the former method the following expression

$$m \int d\tau \sqrt{\dot{x}^2} - \log \langle W[x] \rangle + i \int d\tau a_\mu^{\text{ex}} \dot{x}^\mu \quad (3.14)$$

appears in the exponential in (3.4). In the latter method, the factor (3.14) is replaced by  $S_{\text{NG}} + S_{B_2}$ . That is, the particle action and the VEV of the Wilson loop are replaced by the NG string action  $S_{\text{NG}}$ . Then the NS-NS two-form in  $S_{B_2}$  is interpreted as an external electric field on the probe D3-brane via the following relation,

$$T_{\text{F}} B_{01} = E.$$

In the 't Hooft limit, the classical analysis is sufficient on the string-theory side. To begin with, we construct a classical solution whose boundary is a circular Wilson loop on the probe D3-brane by taking the following ansatz (See Fig. 2) :

$$\begin{aligned} x^0 &= x(\sigma) \cos \tau, & x^1 &= x(\sigma) \sin \tau, & x^2 &= x^3 = 0, \\ r &= r(\sigma), & x^2 + \left(\frac{L^2}{r}\right)^2 &= R^2 + \left(\frac{L^2}{r_0}\right)^2, \end{aligned} \quad (3.15)$$

where  $R$  is the radius of the circle on the probe D3-brane<sup>7</sup>. The range of  $\tau$  is  $0 \leq \tau < 2\pi$ . Note that the coupling to a constant NS-NS 2-form does not change the classical equation of motion. Hence the classical solution is given by

$$x(\sigma) = \frac{1}{\cosh \sigma} \sqrt{R^2 + \left(\frac{L^2}{r_0}\right)^2}, \quad r(\sigma) = \frac{L^2}{\tanh \sigma \sqrt{R^2 + (L^2/r_0)^2}}. \quad (3.16)$$

---

<sup>7</sup> Note that  $x^0 = x(\sigma) \cos(n\tau)$ ,  $x^1 = x(\sigma) \sin(n\tau)$  with  $n \geq 2$  satisfy the circular ansatz (3.15). However, the contributions of the solutions with  $n \geq 2$  are suppressed in comparison to the one with  $n = 1$ , and hence we will concentrate on the ansatz (3.15).

Here the range of  $\sigma$  is taken as  $\sigma_0 \leq \sigma < \infty$  and  $\sinh \sigma_0 = L^2/Rr_0$ .

The next is to argue the boundary condition on the probe D3-brane. Note that the NS-NS 2-form is relevant to the boundary condition, while it is blind to the equations of motion. In the present case, one needs to impose the following mixed boundary condition:

$$\sqrt{\det G} G^{\alpha\sigma} g_{MN} \frac{\partial x^M}{\partial \sigma^\alpha} - B_{MN} \frac{\partial x^M}{\partial \tau} = 0. \quad (3.17)$$

This boundary condition determines the radius  $R$  like

$$R = \frac{L^2}{r_0} \sqrt{\left(\frac{E_c}{E}\right)^2 - 1}. \quad (3.18)$$

Here we have defined  $E_c$  as

$$E_c \equiv T_{\text{F}} \frac{r_0^2}{L^2} = \frac{2\pi m^2}{\sqrt{\lambda}}. \quad (3.19)$$

Note that the classical solution does not exist when  $E$  is larger than  $E_c$ . It is also possible to derive the relation (3.18) by taking a variation of  $S_{\text{cl}}$  with respect to  $R$ , as originally argued in the work [13].

Finally, by substituting the classical solution (3.16) to the string action, the production rate is evaluated as

$$\Gamma \sim \exp \left[ -\frac{\sqrt{\lambda}}{2} \left( \sqrt{\frac{E_c}{E}} - \sqrt{\frac{E}{E_c}} \right)^2 \right] = \exp \left( -\frac{\pi m^2}{E} + \sqrt{\lambda} - \frac{E}{\pi m^2} \right). \quad (3.20)$$

The first and second terms in the exponential are the same as the expression (3.6). The third term should be regarded as a correction term and can be ignored under the weak-field condition  $E \ll m^2$ . In fact, the classical action vanishes when  $E = E_c$ .

It is worth comparing the result (3.19) with the critical electric field derived from the DBI action of the probe D3-brane. Here we will work in the Lorentzian signature. The DBI action in the bulk AdS is given by

$$S_{\text{DBI}} = -T_{\text{D3}} \frac{r_0^4}{L^4} \int d^4x \sqrt{1 - \frac{(2\pi\alpha')^2 L^4}{r_0^4} E^2}, \quad (3.21)$$

where the D3-brane tension is given by

$$T_{\text{D3}} = \frac{1}{g_s (2\pi)^3 \alpha'^2}.$$

One can see that the DBI action is ill-defined when  $E > 2\pi m^2/\sqrt{\lambda}$ . Thus, the critical electric field is given by

$$E_c^{\text{DBI}} = \frac{2\pi m^2}{\sqrt{\lambda}}. \quad (3.22)$$

This completely agrees with the result (3.19).

As we have seen so far, Semenoff and Zarembo's proposal works well on the critical electric field and has resolved the two unsatisfactory points raised at the end of sec. 3.1. Then the production rate (3.20) coincides with the result (3.6) computed with the world-line instanton method, under the weak-field condition  $E \ll m^2$ . Thus it seems likely that there would be no problem for the exponential factor.

However, it has not succeeded yet to evaluate the prefactor of the exponential with the present holographic set-up. The difficulty comes from the fact there is a subtlety in regularizing quantum fluctuations around a circular Wilson loop, in comparison to a straight line. In fact, some trials have already been done [37–40], but unfortunately none of them has succeeded.

Finally, it is useful to comment on some generalizations of Semenoff and Zarembo's work [13]. One may consider the finite temperature case [20, 31] by following the works [41, 42]. Bolognesi et. al. [31] argued the pair creation of monopole and anti-monopole in an external magnetic field. Some cases with external electro-magnetic fields are also studied [32].

## 4 The Schwinger effect in a confining gauge theory

So far, we have studied a holographic description of the Schwinger effect in the Coulomb phase. An interesting direction is to consider the Schwinger effect in the confining phase by generalizing the previous set-up. This section is devoted to the study of the Schwinger effect in a confining gauge theory by employing a holographic approach [14–16].

It would be important to motivate the readers to study the Schwinger effect in the confining phase, before going to the detail. Recently, QCD in strong external fields has been intensively studied to explain experimental data of RHIC and LHC. In these experiments, a extremely strong magnetic field is induced, because colliding nuclei have large electric charge and move very fast. This strong magnetic field may have a visible effect on the nuclear dynamics. Apart from the magnetic field, a strong electric field is also

created around the nuclei as well as a strong color field. Thus, to capture the underlying physics concerned with the experiments, it is inevitable to study the QCD dynamics in the presence of strong external fields. As a matter of course, the Schwinger effect in the confining phase is included in this direction.

We will utilize a holographic approach to study the Schwinger effect, but one may wonder whether the lattice formulation would be enough to study it. In the presence of an external electric field, one encounter a notorious sign problem and hence it is quite difficult to use the lattice formulation in general. Some researchers may hesitate to borrow a holographic computation. But one cannot disguise the fact that there is no definite method to tackle this issue instead of it, at least so far. It would be quite useful to capture qualitative pictures of the Schwinger effect in the confining phase even by employing the AdS/CFT. In fact, one can see quantitative predictions as well as qualitative understanding by pursuing this direction.

## 4.1 Set-up

First of all, let us introduce the set-up to study the Schwinger effect in the confining phase. For this purpose, the bulk AdS<sub>5</sub> has to be replaced with another confining background with a dimensionful parameter. There are lots of backgrounds dual to confining gauge theories. A simple example is an AdS<sub>5</sub> soliton background (often called a confining D3-brane background)<sup>8</sup>.

The metric of the AdS<sub>5</sub> soliton background is given by

$$ds^2 = \frac{L^2}{z^2} \left[ -(dx^0)^2 + \sum_{i=1}^2 (dx^i)^2 + f(z)(dx^3)^2 + \frac{dz^2}{f(z)} \right] + L^2 d\Omega_5^2, \\ f(z) = 1 - \left( \frac{z}{z_t} \right)^4. \quad (4.1)$$

Now the radial direction is described by  $z$  and a scalar function  $f(z)$  contains a constant parameter  $z_t$ . Then the geometry is cut off at  $z = z_t$  and the conformal boundary is at  $z = 0$ . The parameter  $z_t$  has the dimension of length and the inverse has the dimension of energy. Hence  $1/z_t$  gives rise to the confining string tension on the dual gauge-theory side. As  $z_t \rightarrow \infty$ ,  $f(z) \rightarrow 1$  and the usual AdS<sub>5</sub> geometry is reproduced.

---

<sup>8</sup> In this review, we will concentrate on an AdS<sub>5</sub> soliton background for simplicity, but it would be easy to generalize the present analysis to the other confining backgrounds by following the work [15].

As another point, the  $x^3$ -direction is compactified on a circle  $S^1$  with the radius  $R = \pi z_t$ . Hence the limit  $z_t \rightarrow \infty$  corresponds to the decompactification limit  $R \rightarrow \infty$ . Anyway, the dual gauge theory lives on  $\mathbb{R}^{1,2} \times S^1$  rather than  $\mathbb{R}^{1,3}$ . Thus the dual gauge theory cannot be regarded as the usual confining gauge theory in  $1 + 3$  dimensions. Still, however, it would be possible to extract qualitative behaviors by examining the  $\text{AdS}_5$  soliton background. The results obtained here would be a key ingredient towards the study in the real QCD.

## 4.2 Potential analysis

Let us first study the Schwinger effect in the confining phase from the viewpoint of potential analysis. Naively, the Schwinger effect could be argued with the modified potential

$$V_{\text{tot}}(x) = 2m + V(x) - Ex + \sigma_{\text{st}}x. \quad (4.2)$$

Here the modification is that a confining potential with the string tension  $\sigma_{\text{st}}$  is added as well as the usual potential analysis. An important observation is that the string tension  $\sigma_{\text{st}}$  and the electric field  $E$  compete with each other. When  $\sigma_{\text{st}} > E$ , the potential diverges as  $x \rightarrow \infty$  and hence the Schwinger effect would not occur. On the other hand, when  $\sigma_{\text{st}} < E$ , the situation is not so different from the Coulomb phase and the qualitative behavior would be almost the same as the previous.

In the holographic set-up, it is necessary to evaluate the VEV of a rectangular Wilson loop for the quark anti-quark potential. It can be computed with the minimal surface of a string attaching to the loop on the probe D3-brane embedded in the  $\text{AdS}_5$  soliton background.

In this subsection, we will work with

$$r = \frac{L^2}{z}$$

as the radial coordinate, following the notation of our article [14]. Hereafter, we move to the Euclidean signature. The probe D3-brane is supposed to be at  $r = r_0$ . We impose the following ansatz for the rectangular Wilson loop (See Fig. 3):

$$x^0 = \tau, \quad x^1 = \sigma, \quad r = r(\sigma). \quad (4.3)$$

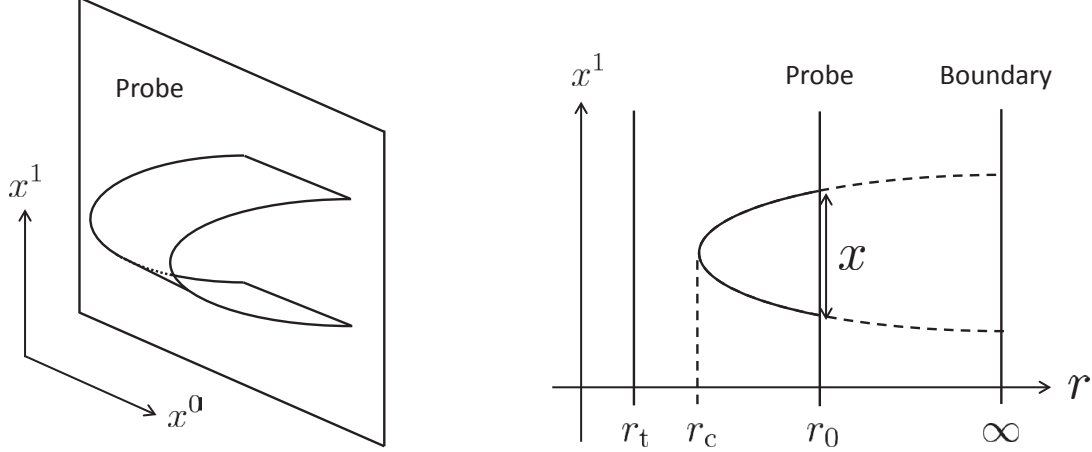


Figure 3: The configuration of the string world-sheet for the quark and anti-quark potential.

The NG part of the string action is

$$\mathcal{L} = \sqrt{\det G} = \sqrt{\frac{1}{1 - r_t^4/r^4} \left( \frac{dr}{d\sigma} \right)^2 + \frac{r^4}{L^4}}. \quad (4.4)$$

Since the Lagrangian does not depend on  $\sigma$  explicitly, the Hamiltonian

$$\frac{\partial \mathcal{L}}{\partial(\partial_\sigma r)} \partial_\sigma r - \mathcal{L} \quad (4.5)$$

is conserved. When we impose the boundary condition at the tip of the minimal surface like

$$\frac{dr}{d\sigma} = 0, \quad r = r_c \quad (r_t < r_c < r_0), \quad (4.6)$$

the conserved quantity becomes

$$\frac{r^4}{\sqrt{\frac{1}{1 - r_t^4/r^4} \left( \frac{dr}{d\sigma} \right)^2 + \frac{r^4}{L^4}}} = \text{const.} \equiv r_c^2 L^2. \quad (4.7)$$

By rewriting the conserved quantity, we obtain

$$\frac{dr}{d\sigma} = \frac{1}{L^2} \sqrt{(r^4 - r_t^4) \left( \frac{r^4}{r_c^4} - 1 \right)}. \quad (4.8)$$

By integrating the expression (4.8), the distance between a quark and an anti-quark,  $x$ , is given by

$$x = \frac{2L^2}{r_0 a} \int_1^{1/a} \frac{dy}{\sqrt{(y^4 - 1)(y^4 - (b/a)^4)}}, \quad (4.9)$$

where we have defined dimensionless quantities as

$$y \equiv \frac{r}{r_c}, \quad a \equiv \frac{r_c}{r_0}, \quad b \equiv \frac{r_t}{r_0}.$$

The sum of the potential energy and static energy is evaluated as

$$V_{\text{PE+SE}} = 2T_{\text{F}} \int_0^{x/2} d\sigma \mathcal{L} = 2T_{\text{F}} r_0 a \int_1^{1/a} dy \frac{y^4}{\sqrt{(y^4 - 1)(y^4 - (b/a)^4)}}. \quad (4.10)$$

Here  $x$  is a function of  $a$ , and hence the potential is a function of  $x$  through  $a$ .

For large  $x$  limit (i.e.  $a \rightarrow b$  limit), the sum of the potential energy and static energy behaves as

$$V_{\text{PE+SE}} = T_{\text{F}} \left( \frac{r_0}{L} \right)^2 b^2 x + 2T_{\text{F}} r_0 b \left( \frac{1}{b} - 1 \right). \quad (4.11)$$

The first term is the quark and anti-quark potential with a confining string tension

$$\sigma_{\text{st}} = T_{\text{F}} \left( \frac{r_t}{L} \right)^2,$$

and the second term is static mass of quark and anti-quark

$$2T_{\text{F}}(r_0 - r_t) = 2m_{\text{W}}.$$

By including the energy coming from the external electric field, the total potential is rewritten into an integral representation,

$$\begin{aligned} V_{\text{tot}} &= V_{\text{PE+SE}} - Ex \\ &= 2T_{\text{F}} r_0 a \int_1^{1/a} dy \frac{y^4}{\sqrt{(y^4 - 1)(y^4 - (b/a)^4)}} \\ &\quad - \frac{2T_{\text{F}} r_0 \alpha}{a} \int_1^{1/a} \frac{dy}{\sqrt{(y^4 - 1)(y^4 - (b/a)^4)}}, \end{aligned} \quad (4.12)$$

where we have introduced a dimensionless electric field  $\alpha$

$$\alpha \equiv \frac{E}{E_c}, \quad E_c \equiv T_{\text{F}} \frac{r_0^2}{L^2}. \quad (4.13)$$

$E_c$  is the critical electric field obtained from the DBI action. In the following, we define a dimensionless electric field  $\alpha$  normalized by  $E_c$ .

The total potential is plotted in Fig. 4 as a function of  $x$ . Figure 4 shows the existence of two critical electric fields. The first one is

$$E = E_s \equiv \sigma_{\text{st}} \quad (\alpha = b^2), \quad (4.14)$$

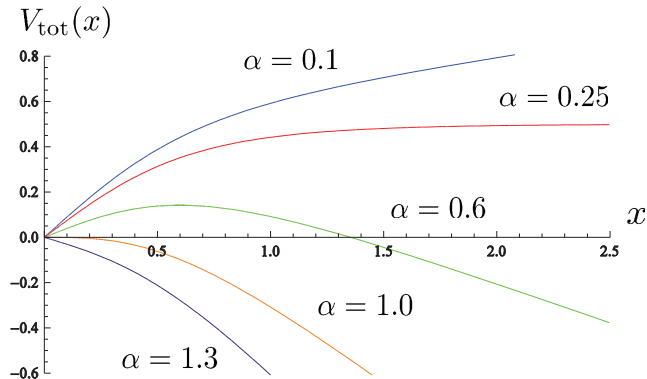


Figure 4: The plots of the total potential with  $b = 0.5$  and  $2L^2/r_0 = 2T_{\text{F}}r_0 = 1$ . The blue line is for  $\alpha = 0.1$ . There is no zero other than the origin and hence the Schwinger effect does not occur. The red line is for  $\alpha = 0.25$ . This value corresponds to  $b^2 = 0.25$  and the potential becomes flat as  $x \rightarrow \infty$ . For the values of  $\alpha$  between 0.25 and 1.0, the potential barrier is formed and the Schwinger effect can occur as a tunneling process. When  $\alpha = 1.0$  (the orange line), the barrier just vanishes and the system becomes unstable catastrophically.

and the second is

$$E = E_c \quad (\alpha = 1). \quad (4.15)$$

When the electric field is smaller than the confining string tension, the pair production is prohibited because the potential does not dump at infinity. When the electric field is larger than it, it is allowed as a tunneling process. Thus, at the first critical electric field, a confinement/deconfinement transition starts. As a side remark, a similar behavior of the phenomenological potential in a confining theory has been argued by using a lattice formulation [43].

The second critical electric field is the same as the critical electric field obtained in the Coulomb phase. That is, the vacuum becomes unstable catastrophically above this value of the electric field. Note that this qualitative behavior can also be understood analytically. For the detail, see the works [14, 15, 20].

Here we are mainly concerned with the long-distance behavior of the potential. But it would be worth commenting on the short-distance behavior. As shown in Fig. 4, the potential becomes zero at the origin, in comparison to the usual potential analysis. This is just because the Coulomb potential is modified on the probe D3-brane sitting at an



intermediate position in the bulk. The modified Coulomb potential was originally argued by Kabat and Lifschytz [44].

### 4.3 The production rate

In this subsection, we will compute the production rate numerically and examine two critical electric fields. Both of the resulting critical values agree with the ones obtained in the potential analysis [14]. Furthermore, we will introduce new exponents associated with the critical behaviors and evaluate the numerical values.

To compute the production rate, one has to evaluate the VEV of a circular Wilson loop on the probe D3-brane. Then the D3-brane is placed at an intermediate position between  $z = z_t$  and  $z = 0$ .

The first is to construct a classical string solution attaching to the circular Wilson loop. Let us suppose the following ansatz:

$$x^0 = x(\sigma) \cos \tau, \quad x^1 = x(\sigma) \sin \tau, \quad z = z(\sigma). \quad (4.16)$$

The other components are set to be zero. Suppose that the world-sheet coordinates  $(\tau, \sigma)$  are restricted to the following range:

$$0 \leq \tau < 2\pi, \quad 0 \leq \sigma \leq \sigma_0.$$

Then boundary conditions for  $x(\sigma)$  and  $z(\sigma)$  are imposed like

$$x(0) = 0, \quad x(\sigma_0) = R, \quad z(0) = z_c, \quad z(\sigma_0) = z_0. \quad (4.17)$$

The configuration is depicted in Fig. 5.

In addition, a constant field  $B_2$  is set to be

$$T_F B_{01} \equiv E.$$

This  $B_2$  field induces an external electric field on the probe D3-brane. Then the resulting NG action and the coupling to  $B_2$  are given by, respectively,

$$S_{\text{NG}} = 2\pi L^2 T_F \int_0^R dx \frac{x}{z^2} \sqrt{1 + \frac{z'^2}{f(z)}}, \quad (4.18)$$

$$S_{B_2} = -2\pi T_F B_{01} \int_0^R dx x = -\pi E R^2. \quad (4.19)$$

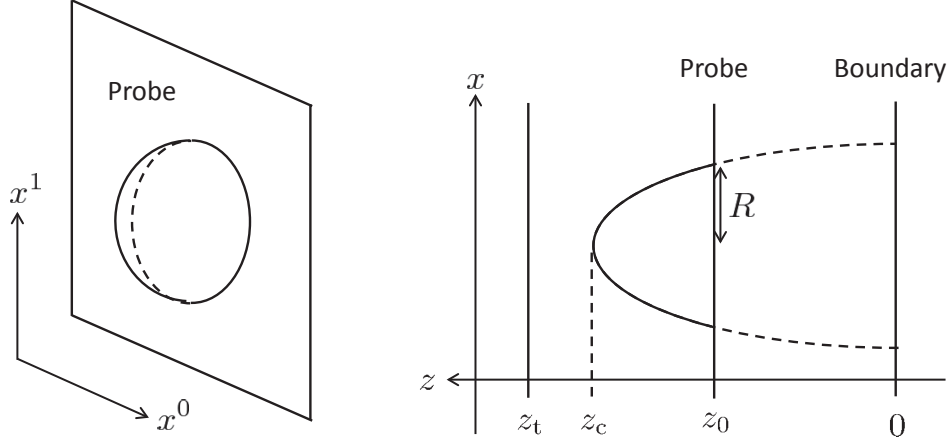


Figure 5: The configuration of the string world-sheet for the Schwinger pair production.

Here we take that  $\sigma = x(\sigma)$  with a diffeomorphism invariance. The prime denotes the derivative with respect to  $x$ .

. Then the equation of motion for  $z(x)$  is obtained as

$$z' + \frac{2xf(z)}{z} + xz'' - \frac{xz'^2}{2f(z)} \frac{df}{dz}(z) + \frac{z'^3}{f(z)} + \frac{2xz'^2}{z} = 0. \quad (4.20)$$

In the presence of the  $B_2$  field, the boundary condition on the probe D3-brane becomes the mixed boundary condition:

$$z' = -\sqrt{f(z) \left( \frac{1}{\alpha^2} - 1 \right)} \Big|_{z=z_0}. \quad (4.21)$$

Here  $\alpha$  is a dimensionless electric field defined in (4.13).

It is difficult to solve analytically the differential equation (4.20) with the boundary condition (4.21). Hence let us solve it numerically and study the behavior of  $z(x)$ . As a result, we will show the existence of two critical electric fields and the consistency of the values with the ones obtained from the potential analysis in subsec. 4.2. Hereafter, we take that

$$\lambda = 100 \quad (2\pi T_F L^2 = 10),$$

to validate the holographic description (i.e., large  $\lambda$ ).

For some values of  $z_0/z_t$ , numerical results are shown in Fig. 6. The left figure shows exponential suppression factors, and the right one is plots of the classical action. Typically, the suppression factors tend to vanish below certain values of  $\alpha$  (i.e.,  $E = E_c$ ), depending

on values of  $z_0/z_t$ . This is the same  $E$ -dependence as in the Coulomb phase. In the case of the confining phase, one can see a new behavior that the classical action diverges (i.e. the exponential factor vanishes) at the value  $E = E_s$ . This result indicates that the Schwinger effect does not occur when  $E < E_s$ . Note that the value of  $E_s$  agrees with the potential analysis as well. As a matter of course, the value of  $E_s$  depends on  $z_0/z_t$ , and  $E_s$  becomes zero as  $z_t \rightarrow \infty$ .

In total, the two critical electric fields  $E_s$  and  $E_c$  have been seen from Fig. 6. These are the same as the ones obtained by the potential analysis in subsec. 4.2,

$$E_c \equiv T_F \frac{L^2}{z_0^2}, \quad E_s \equiv T_F \frac{L^2}{z_t^2}. \quad (4.22)$$

This agreement supports that our numerical results of the production rate are consistent with the previous potential analysis.

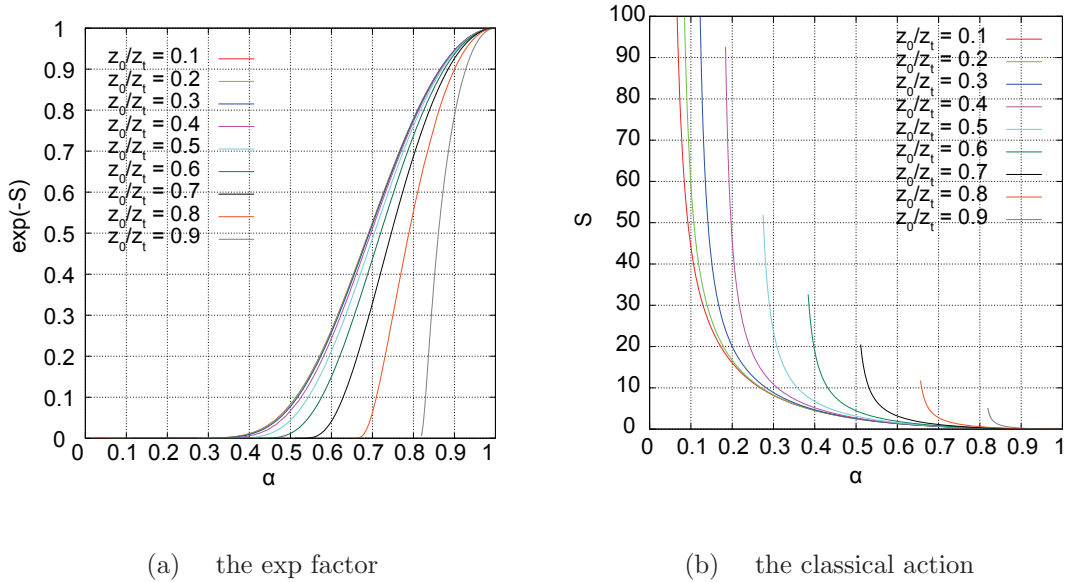


Figure 6: The plots of the exponential factor and the classical action.

## The critical behaviors

Let us examine the critical behaviors of the classical action numerically. We first argue the behavior of the classical action around  $E = E_s$ , by focusing upon the singular behavior. Then the critical behavior around  $E = E_c$  is discussed numerically and analytically. For

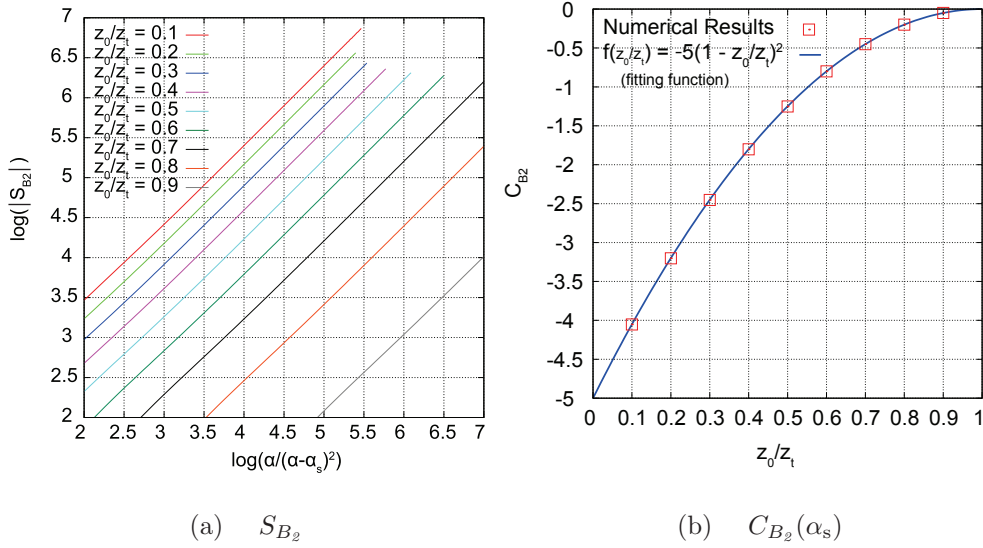


Figure 7: The behaviors of  $S_{B_2}$  and  $C_{B_2}(\alpha_s)$  near  $E = E_s$ .

both critical behaviors, we will introduce new exponents and determine the numerical values.

**i) the critical behavior around  $E = E_s$**

Let us consider the behavior near  $E = E_s$ . The log-log plot of  $S_{B_2}$  shown in Fig. 7 (a) indicates that the  $\alpha$ -dependence of  $S_{B_2}$  may be described by

$$S_{B_2} = \frac{C_{B_2}(\alpha_s) \alpha}{(\alpha - \alpha_s)^2} + \text{the regular}, \quad \alpha_s \equiv \frac{E_s}{E_c}. \quad (4.23)$$

Figure 7 (b) shows that the coefficient  $C_{B_2}(\alpha_s)$  is well approximated by

$$C_{B_2}(\alpha_s) = -\frac{\sqrt{\lambda}}{2}(1 - \sqrt{\alpha_s})^2. \quad (4.24)$$

As a result, by combining (4.19) and (4.23), the behavior of the Wilson loop radius  $R$  near  $E = E_s$  is evaluated as

$$R = \frac{(1 - \sqrt{\alpha_s})z_0}{\alpha - \alpha_s} + \text{the regular}. \quad (4.25)$$

This result means that  $R$  tends to diverge as  $E \rightarrow E_s + 0$ .

The next is to examine the NG action. The log-log plot shown in Fig. 8 (a) indicates that the  $\alpha$ -dependence of the NG action is approximated by

$$S_{\text{NG}} = \frac{C_{\text{NG}}(\alpha_s) \alpha}{(\alpha - \alpha_s)^2} + \frac{D_{\text{NG}}(\alpha_s)}{\alpha - \alpha_s} + \text{the regular}. \quad (4.26)$$

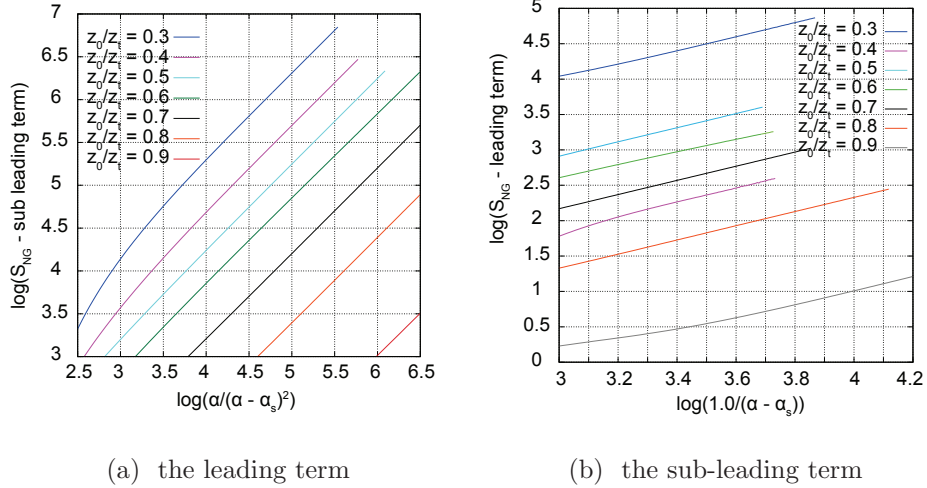


Figure 8: The leading and sub-leading terms of  $S_{\text{NG}}$  near  $E = E_s$ .

Here  $C_{\text{NG}}(\alpha_s)$  and  $D_{\text{NG}}(\alpha_s)$  are scalar functions to be determined.

We should comment on the validity of our numerical results. The plots in Fig. 8 would be valid for  $\alpha_s > 0.1$  because of the limitation of numerical precision. If the accuracy of numerical analysis could be increased, then the lines in Fig. 8 are extended more to the right-hand side.

In total, the total classical action  $S = S_{\text{NG}} + S_{B_2}$  is given by

$$S = \frac{C(\alpha_s)\alpha}{(\alpha - \alpha_s)^2} + \frac{D(\alpha_s)}{\alpha - \alpha_s} + \text{the regular}, \quad (4.27)$$

where we have defined new quantities as

$$C(\alpha_s) \equiv C_{\text{NG}}(\alpha_s) + C_{B_2}(\alpha_s), \quad D(\alpha_s) \equiv D_{\text{NG}}(\alpha_s).$$

Note that  $C(\alpha_s)$  is nonzero for  $\alpha_s \neq 0$ . Therefore, in the deconfining limit  $\alpha_s \rightarrow 0$ , the total action  $S$  becomes

$$S = \frac{C(0) + D(0)}{\alpha} + \text{the regular}. \quad (4.28)$$

Then the following relation should be satisfied,

$$C(0) + D(0) = \frac{\sqrt{\lambda}}{2},$$

However, we have not confirmed this point yet because of the limitation of numerical analysis as mentioned in the last paragraph.

It would be nice to consider the meaning of the power of the singularity. It is associated with the critical behavior and hence may be interpreted as a new critical exponent. Suppose the following divergent form around  $E = E_s$  :

$$S = A(\alpha_s)(\alpha - \alpha_s)^{-\gamma_s} + \dots . \quad (4.29)$$

Now  $\gamma_s$  is a new exponent. Our numerical computation indicates that

$$\gamma_s = 2 .$$

This may be regarded as a non-trivial prediction to the real QCD if this value could be interpolated to QCD via the universality argument. In this sense, it would be significant to check the universality of this exponent for general confining backgrounds.

**ii) the critical behavior around  $E = E_c$**

Let us next discuss the behavior near  $E = E_c$ . The classical action should vanish as  $\alpha \rightarrow 1$ , and hence one can expect the following behavior:

$$S = B(\alpha_s)(1 - \alpha)^{\gamma_c} + \dots . \quad (4.30)$$

Here  $\gamma_c$  is a positive constant to be determined and  $B(\alpha_s)$  is an unknown function. The log-log plot of the classical action is shown in Fig. 9 (a). The result indicates that the exponent  $\gamma_c$  is given by

$$\gamma_c = 2 .$$

Moreover, from Fig. 9 (b), one can determine the asymptotic form of  $B(\alpha_s)$  in the  $\alpha_s \rightarrow 0$  limit. As a result, the resulting classical action has been determined as

$$S = \frac{\sqrt{\lambda}}{2}(1 - \alpha)^2 + \mathcal{O}((1 - \alpha)^3) .$$

Note that this expression completely agrees with the asymptotic form derived from (3.20) analytically. This agreement ensures the consistency of our numerical computations.

## 5 Conclusion and Discussion

We have reviewed the recent progress on a holographic description of the Schwinger effect in the Coulomb phase and the confining phase. The part of the Coulomb phase is mainly

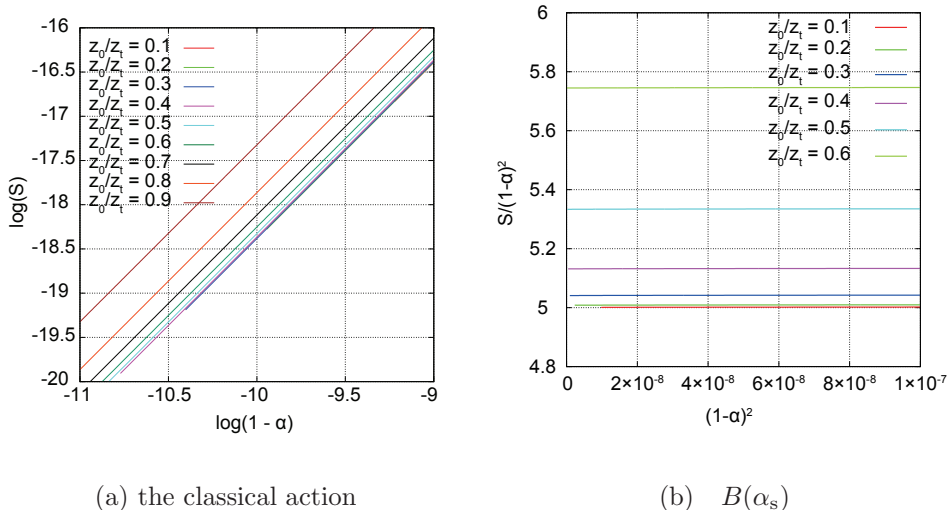


Figure 9: The behavior of the classical action near  $E = E_c$ . The log-log plot in Fig. (a) indicates that  $\gamma_c = 2$  universally. Figure (b) indicates that the coefficient approaches 5 ( $= \frac{\sqrt{\lambda}}{2}$ ) as  $\alpha_s \rightarrow 0$  (Recall that  $\lambda = 100$ ).

based on the seminal work by Semenoff and Zarembo [13]. The part of the confining phase is a summary of a series of our works [14–16].

First, we have introduced the world-line instanton method, which is a standard method to compute the Schwinger production rate. A remarkable point on this method is that the rate can be evaluated even at arbitrary coupling. Then a circular Wilson loop appears in the middle of the computation, in comparison to the weak-coupling analysis. This method is also applicable to the  $\mathcal{N} = 4$  SYM theory through the Higgs mechanism by assuming the heavy quark mass and the weak-field condition. Notably, in this case, a circular 1/2 BPS Wilson loop appears in the formula of the production rate (3.4). The VEV of the Wilson loop is estimated by using the AdS/CFT correspondence. However, there are unsatisfactory points: 1) it seems unlikely that the Schwinger effect occur for very heavy quarks, 2) disagreement of the critical electric fields computed from the production rate and the DBI action of a probe D3-brane.

To resolve this problem, Semenoff and Zarembo improved the AdS/CFT set-up. The probe D3-brane is put at an intermediate position in the bulk  $\text{AdS}_5$ . Then the quark mass becomes arbitrary and the critical electric fields nicely agree. According to this improvement, the production rate is corrected with an additional term, which can be

ignored under the weak-field condition. Note also that the Coulomb potential is modified [20] as well. The critical electric field obtained from the potential analysis also agrees with the results from the production rate and the DBI action.

The holographic method argued in the Coulomb phase has been generalized to confining gauge theories. In this review we have focused upon an AdS<sub>5</sub> soliton background. The potential analysis has been done [14] and it has been shown that there are two kinds of critical behaviors around (1)  $E = E_s$  and (2)  $E = E_c$ . When  $E \leq E_s$ , the Schwinger effect cannot occur due to the confining string tension. In the region with  $E_s < E < E_c$ , it is possible as a tunneling effect as usual. When  $E \geq E_c$ , the vacuum is unstable catastrophically. Finally, the production rate has been evaluated numerically. Then we have introduced new critical exponents associated with the two critical behaviors. The values of the exponents are non-trivial results and might be regarded as a prediction in the real QCD via the universality argument, as in the case of the ratio of the shear viscosity  $\eta$  to the entropy density  $s$ ,  $\eta/s = 1/4\pi$  [45]. Thus it is of importance to check the universality of them for various backgrounds [17]. As a matter of course, it should be significant to reveal the mathematical foundation for the universality by employing the holographic approach discussed here as a compass.

We have concentrated on an AdS soliton background as a confining geometry. As other examples, one may consider  $\mathcal{N} = 2$  supersymmetric QCD and the Sakai-Sugimoto model [46]. The Schwinger effect in the former case has been studied in a series of works [47–49]. As for the latter case, see the recent work [50]. Another holographic Schwinger effect based on the bottom up approach is discussed by Dietrich [51]. It would be significant to study the Schwinger effect in confining theories from various perspectives. It is also interesting to study a holographic description of the Schwinger effect in de Sitter space [52]. It is argued that no pair production occurs in a plane-wave background [53].

We believe that the Schwinger effect in confining gauge theories would be a key ingredient in looking for new aspects of QCD in the presence of extremely strong external fields.



## Acknowledgments

We appreciate K. Hashimoto and H. Suganuma for useful comments and discussion. The work of YS is supported by a Grant-in-Aid for Japan Society for the Promotion of Science (JSPS) Fellows No. 26-1300.

## References

- [1] J. S. Schwinger, “On gauge invariance and vacuum polarization,” *Phys. Rev.* **82** (1951) 664.
- [2] W. Heisenberg and H. Euler, “Consequences of Dirac’s theory of positrons,” *Z. Phys.* **98** (1936) 714 [physics/0605038].
- [3] G. V. Dunne, “Heisenberg-Euler effective Lagrangians: Basics and extensions,” In \*Shifman, M. (ed.) et al.: From fields to strings, vol. 1\* 445-522 [hep-th/0406216].
- [4] A. Casher, H. Neuberger and S. Nussinov, “Chromoelectric Flux Tube Model of Particle Production,” *Phys. Rev. D* **20** (1979) 179.
- [5] J. Ambjorn and R. J. Hughes, “Canonical Quantization In Nonabelian Background Fields. 1.,” *Annals Phys.* **145** (1983) 340.
- [6] M. Gyulassy and A. Iwazaki, “Quark And Gluon Pair Production In  $SU(n)$  Covariant Constant Fields,” *Phys. Lett. B* **165** (1985) 157.2
- [7] L. Alvarez-Gaume and M. A. Vazquez-Mozo, “An invitation to quantum field theory,” *Lect. Notes Phys.* **839** (2012) 1.
- [8] E. S. Fradkin and A. A. Tseytlin, “Quantum String Theory Effective Action,” *Nucl. Phys. B* **261** (1985) 1.
- [9] C. Bachas and M. Porrati, “Pair creation of open strings in an electric field,” *Phys. Lett. B* **296** (1992) 77 [hep-th/9209032].
- [10] J. M. Maldacena, “The large N limit of superconformal field theories and supergravity,” *Adv. Theor. Math. Phys.* **2** (1998) 231 [*Int. J. Theor. Phys.* **38** (1999) 1113]. [arXiv:hep-th/9711200].

- [11] S. S. Gubser, I. R. Klebanov and A. M. Polyakov, “Gauge theory correlators from non-critical string theory,” *Phys. Lett. B* **428** (1998) 105 [arXiv:hep-th/9802109].
- [12] E. Witten, “Anti-de Sitter space and holography,” *Adv. Theor. Math. Phys.* **2** (1998) 253 [arXiv:hep-th/9802150].
- [13] G. W. Semenoff and K. Zarembo, “Holographic Schwinger Effect,” *Phys. Rev. Lett.* **107** (2011) 171601 [arXiv:1109.2920 [hep-th]].
- [14] Y. Sato and K. Yoshida, “Holographic Schwinger effect in confining phase,” *JHEP* **1309** (2013) 134 [arXiv:1306.5512 [hep-th]].
- [15] Y. Sato and K. Yoshida, “Universal aspects of holographic Schwinger effect in general backgrounds,” *JHEP* **1312** (2013) 051 [arXiv:1309.4629 [hep-th]].
- [16] D. Kawai, Y. Sato and K. Yoshida, “The Schwinger pair production rate in confining theories via holography,” *Phys. Rev. D* **89** (2014) 101901 [arXiv:1312.4341 [hep-th]].
- [17] Y. Kinar, E. Schreiber and J. Sonnenschein, “ $Q\bar{Q}$  potential from strings in curved space-time: Classical results,” *Nucl. Phys. B* **566** (2000) 103 [hep-th/9811192].
- [18] J. Sonnenschein, “What does the string / gauge correspondence teach us about Wilson loops?,” hep-th/0003032.
- [19] J. Sonnenschein, “Stringy confining Wilson loops,” hep-th/0009146.
- [20] Y. Sato and K. Yoshida, “Potential Analysis in Holographic Schwinger Effect,” *JHEP* **1308** (2013) 002 [arXiv:1304.7917 [hep-th]].
- [21] G. T. Horowitz and R. C. Myers, “The AdS / CFT correspondence and a new positive energy conjecture for general relativity,” *Phys. Rev. D* **59** (1998) 026005 [hep-th/9808079].
- [22] I. K. Affleck, O. Alvarez and N. S. Manton, “Pair Production At Strong Coupling In Weak External Fields,” *Nucl. Phys. B* **197** (1982) 509.
- [23] G. V. Dunne and C. Schubert, “Worldline instantons and pair production in inhomogeneous fields,” *Phys. Rev. D* **72** (2005) 105004 [hep-th/0507174].

- [24] G. V. Dunne, Q. -h. Wang, H. Gies and C. Schubert, “Worldline instantons. II. The Fluctuation prefactor,” *Phys. Rev. D* **73** (2006) 065028 [hep-th/0602176].
- [25] I. K. Affleck and N. S. Manton, “Monopole Pair Production In A Magnetic Field,” *Nucl. Phys. B* **194** (1982) 38.
- [26] A. S. Gorsky, K. A. Saraikin and K. G. Selivanov, “Schwinger type processes via branes and their gravity duals,” *Nucl. Phys. B* **628** (2002) 270 [hep-th/0110178].
- [27] A. Karch and A. O’Bannon, “Metallic AdS/CFT,” *JHEP* **0709** (2007) 024 [arXiv:0705.3870 [hep-th]].
- [28] J. Erdmenger, R. Meyer and J. P. Shock, “AdS/CFT with flavour in electric and magnetic Kalb-Ramond fields,” *JHEP* **0712** (2007) 091 [arXiv:0709.1551 [hep-th]].
- [29] T. Albash, V. G. Filev, C. V. Johnson and A. Kundu, “Quarks in an external electric field in finite temperature large N gauge theory,” *JHEP* **0808** (2008) 092 [arXiv:0709.1554 [hep-th]].
- [30] ’t Hooft, “A planar diagram theory for strong interactions,” *Nucl. Phys. B* **72** (1974) 461.
- [31] S. Bolognesi, F. Kiefer and E. Rabinovici, “Comments on Critical Electric and Magnetic Fields from Holography,” *JHEP* **1301** (2013) 174 [arXiv:1210.4170 [hep-th]].
- [32] Y. Sato and K. Yoshida, “Holographic description of the Schwinger effect in electric and magnetic fields,” *JHEP* **1304** (2013) 111 [arXiv:1303.0112 [hep-th]].
- [33] N. Drukker, D. J. Gross and H. Ooguri, “Wilson loops and minimal surfaces,” *Phys. Rev. D* **60** (1999) 125006 [hep-th/9904191].
- [34] S. -J. Rey and J. -T. Yee, “Macroscopic strings as heavy quarks in large N gauge theory and anti-de Sitter supergravity,” *Eur. Phys. J. C* **22** (2001) 379 [hep-th/9803001].
- [35] J. M. Maldacena, “Wilson loops in large N field theories,” *Phys. Rev. Lett.* **80** (1998) 4859 [hep-th/9803002].

- [36] D. E. Berenstein, R. Corrado, W. Fischler and J. M. Maldacena, “The Operator product expansion for Wilson loops and surfaces in the large N limit,” *Phys. Rev. D* **59** (1999) 105023 [hep-th/9809188].
- [37] N. Drukker, D. J. Gross and A. A. Tseytlin, “Green-Schwarz string in  $AdS_5 \times S^5$ : Semiclassical partition function,” *JHEP* **0004** (2000) 021 [hep-th/0001204].
- [38] M. Sakaguchi and K. Yoshida, “A Semiclassical string description of Wilson loop with local operators,” *Nucl. Phys. B* **798** (2008) 72 [arXiv:0709.4187 [hep-th]].
- [39] J. Ambjorn and Y. Makeenko, “Remarks on Holographic Wilson Loops and the Schwinger Effect,” *Phys. Rev. D* **85** (2012) 061901 [arXiv:1112.5606 [hep-th]].
- [40] C. Kristjansen and Y. Makeenko, “More about One-Loop Effective Action of Open Superstring in  $AdS_5 \times S^5$ ,” *JHEP* **1209** (2012) 053 [arXiv:1206.5660 [hep-th]].
- [41] E. Witten, “Anti-de Sitter space, thermal phase transition, and confinement in gauge theories,” *Adv. Theor. Math. Phys.* **2** (1998) 505 [hep-th/9803131].
- [42] G. T. Horowitz and A. Strominger, “Black strings and P-branes,” *Nucl. Phys. B* **360** (1991) 197.
- [43] A. Yamamoto, “Lattice QCD with strong external electric fields,” *Phys. Rev. Lett.* **110** (2013) 112001 [arXiv:1210.8250 [hep-lat]].
- [44] D. N. Kabat and G. Lifschytz, “A Note on the Coulomb branch of SUSY Yang-Mills,” *Phys. Lett. B* **633** (2006) 641 [hep-th/0511226].
- [45] G. Policastro, D. T. Son and A. O. Starinets, “The Shear viscosity of strongly coupled  $N=4$  supersymmetric Yang-Mills plasma,” *Phys. Rev. Lett.* **87** (2001) 081601 [hep-th/0104066].
- [46] T. Sakai and S. Sugimoto, “Low energy hadron physics in holographic QCD,” *Prog. Theor. Phys.* **113** (2005) 843 [hep-th/0412141]; “More on a holographic dual of QCD,” *Prog. Theor. Phys.* **114** (2005) 1083 [hep-th/0507073].
- [47] K. Hashimoto and T. Oka, “Vacuum Instability in Electric Fields via AdS/CFT: Euler-Heisenberg Lagrangian and Planckian Thermalization,” *JHEP* **10** (2013) 116 [arXiv:1307.7423 [hep-th]].

- [48] K. Hashimoto, T. Oka and A. Sonoda, “Magnetic instability in AdS/CFT: Schwinger effect and Euler-Heisenberg Lagrangian of supersymmetric QCD,” JHEP **1406** (2014) 085 [arXiv:1403.6336 [hep-th]].
- [49] K. Hashimoto, S. Kinoshita, K. Murata and T. Oka, “Electric Field Quench in AdS/CFT,” JHEP **1409** (2014) 126 [arXiv:1407.0798 [hep-th]].
- [50] K. Hashimoto, T. Oka and A. Sonoda, “Electromagnetic instability in holographic QCD,” arXiv:1412.4254 [hep-th].
- [51] D. D. Dietrich, “Worldline holographic Schwinger effect,” Phys. Rev. D **90** (2014) 045024 [arXiv:1405.0487 [hep-ph]].
- [52] W. Fischler, P. H. Nguyen, J. F. Pedraza and W. Tangarife, “Holographic Schwinger effect in de Sitter space,” arXiv:1411.1787 [hep-th].
- [53] M. Sakaguchi, H. Shin and K. Yoshida, “No pair production of open strings in a plane-wave background,” Phys. Rev. D **90** (2014) 6, 066009 [arXiv:1402.2048 [hep-th]].